Neutron and X-ray scattering for biophysics and biotechnology: examples of self-assembled lipid systems

Thad A. Harroun,*[a] Norbert Kučerka,[b] Mu-Ping Nieh[b] and John Katsaras*[b]

Received 5th November 2008, Accepted 3rd April 2009
First published as an Advance Article on the web 27th May 2009
DOI: 10.1039/b819799g

Membranes that surround cells and separate their contents from the external environment are ubiquitous in biological systems. These membranes are organized assemblies consisting mainly of lipids and proteins, and are highly selective permeability barriers which control the flow of information between cells and their environment. It is accepted that the lipid bilayer is the underlying structure of most, if not all, biomembranes. As such, over the years scientists have exerted much effort in studying lipid bilayers and their biological relevance in hopes of understanding the functional mechanisms taking place at membrane interfaces. Neutron and X-ray scattering techniques are powerful tools for the characterization of the structure and dynamics of biomimetic systems as they provide unique access to microscopic structure and dynamics at length scales ranging from microns to intermolecular and/or atomic distances. The optimization of instruments and preparation techniques, as well as the new possibilities offered by protein deuteration, have opened up new avenues for the study of lipid/protein interactions that were not previously possible. One can now look at the insertion of biomolecules into membranes and accurately determine the structure as well as the dynamics of the interaction. To illustrate the usefulness of diffraction and scattering techniques with regard to biologically relevant systems, we review some of the leading edge studies that have taken place over the last couple of years in which these scattering techniques have played a central role.

1 Introduction

There are numerous experimental techniques that are suitable for the study of the physical chemistry of self assembled lipid dispersions at the microscopic level. Microscopic techniques, including optical and transmission electron microscopies, provide direct information on phases and structures ranging from the micron to nanometre length scale. However, practically speaking only with optical microscopy can samples be studied *in situ* under biologically relevant or other interesting conditions, although at the expense of spatial resolution. On the other hand, scanning probes such as scanning tunneling, atomic force and scanning electron microscopies provide highly detailed information, but are limited to probing the sample's surface. In contrast, scattering techniques allow for the *in situ* manipulation

[a]*Physics Department, Brock University, St. Catharines, Ontario, Canada. E-mail: tharroun@brocku.ca*
[b]*Canadian Neutron Beam Centre, Steacie Institute for Molecular Sciences National Research Council, Chalk River Laboratories, Chalk River, Ontario, Canada. E-mail: John.Katsaras@nrc.gc.ca*

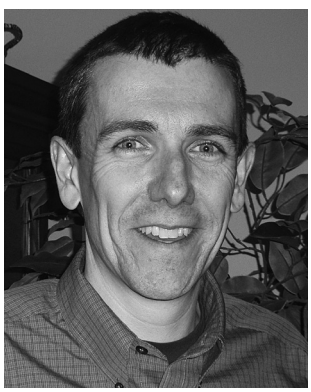

Thad A. Harroun

Thad A. Harroun is currently an Assistant Professor of Physics at Brock University (Ontario, Canada), prior to which he was a post-doctoral fellow with Jeremy Bradshaw (University of Edinburgh), and later on as a research associate with J. Katsaras (NRC). He received his PhD from Rice University (Texas, USA) under the direction of H.W. Huang, studying the effect of peptides on lipid bilayers. Over the years, he has collaborated extensively with researchers at neutron and synchrotron facilities in North America, Europe, and Asia.

Norbert Kučerka

Norbert Kučerka joined the Canadian Neutron Beam Centre (CNBC) in 2006 as a National Science and Engineering Council (NSERC) visiting fellow with J. Katsaras, later becoming research associate. Prior to coming to Canada he was a post-doctoral fellow with J.F. Nagle (Carnegie-Mellon University). He received his PhD from Comenius University (Bratislava, Slovakia) under the direction of P. Balgavý studying lipid unilamellar vesicles with small angle neutron scattering techniques. Presently, his work is focused on determining the structure of model membranes and understanding their highly complex behaviour.

of samples, but more importantly, they provide quantitative data on the distribution of structural features, their sizes, shapes and correlation lengths.

Scattering is a broad term used to describe the constructive interference of waves scattered, or reflected, from atoms at different angles from the direction of the incoming wave. Any sub micron sized objects formed by the aggregation or self assembly of the constituent molecules (*e.g.*, lipids), scatter waves simply through the basic physical interactions of the wave with the atoms—whether electromagnetic waves of X-rays or the quantum wave properties of a particle, such as a neutron or electron.

The geometrical description of scattering and diffraction is based on the idea of reciprocal space. Put simply, an incident beam of photons or neutrons scatters from atoms within the sample. The spatial and temporal correlation of atoms to each other gives rise to constructive and destructive interference in the direction of the detector, as shown in Fig. 1.

All scattering instruments create beams with a well defined direction of incidence $\vec{k}_i$, a vector in the laboratory frame of reference whose length is $|\vec{k}_i| = 2\pi/\lambda$, where λ is the wavelength of the electromagnetic (EM) radiation, or the de Broglie wavelength of the neutron $\lambda = \hbar/p$, where p is the non relativistic neutron momentum. According to particle-wave dualism, neutrons obey the same laws as electromagnetic radiation waves, and they both interact with matter in similar ways (*i.e.*, reflection, refraction and diffraction).

Scattering instruments measure the intensity of the interaction with matter at well defined directions $\vec{k}_f$. Defining the change in the momentum of the scattered photons or particles due to their interaction with the sample as $\vec{q} = \vec{k}_f - \vec{k}_i$, all scattering is mapped into "reciprocal space" by the scattering function $I_m = I_0|S(\vec{q})|^2$. Here, I_m is the measured intensity of radiation in a direction $\vec{k}_f$, and I_0 is the incident intensity. When the detector is in the direction where the reciprocal space vector $\vec{q}$ is made parallel with spatially correlated atoms, constructive interference results and a higher intensity is recorded (see Fig. 1).

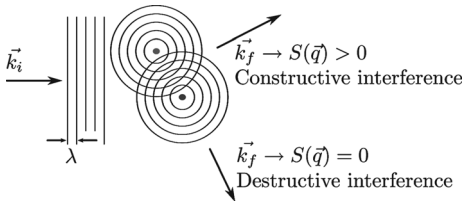

Fig. 1 The principle of diffraction is illustrated by considering wavefronts incident and scattered from atoms within a sample. The frame of reference is the laboratory; the scattering instrument creates beams of well defined direction and wavelength (*i.e.*, $\vec{k}_i$). Two centers of scattering are shown. These could be electron clouds for X-ray scattering, or atomic nuclei in the case of neutron scattering. A detector measures the intensity of scattered particles, $|S(\vec{q})|^2$, in different directions, $\vec{k}_f$, where $\vec{q} = \vec{k}_f - \vec{k}_i$. In the case of constructive interference, a signal is measured, $S(\vec{q}) > 0$. Where there is destructive interference, $S(\vec{q}) = 0$, the signal is zero. Examples of how $S(\vec{q})$ typically appears in various scattering methods are shown in subsequent figures.

The scattering function has the same form for both EM and neutron radiation

$$S(\vec{q}) = \frac{1}{N}\left|\sum_i f_i e^{i\vec{q}\cdot\vec{r}_i}\right|^2 \quad (1)$$

where the sum is over all N atoms in the sample located at positions $\vec{r}_i$. The strength of the interaction between atom and probe is expressed *via* the term f_i, which for X-rays is the Thomson scattering factor, whereby the atom's electrons are considered to be moving freely in "clouds" of electron density.

For neutrons, f_i is the "scattering length", often written as b_i, and is related to the probability for scattering the neutron into the direction of the detector, more commonly called the scattering cross section; $\sigma_{\text{total}} = 4\pi b^2$ (for further details the reader is referred to ref. 1). If we include inelastic scattering, then the scattered beam may change its energy E_f as well as its momentum $\vec{k}_f$. In this case, a change in energy

Mu-Ping Nieh

Mu-Ping Nieh is an Associate Research Officer with the National Research Council of Canada (NRC). Prior to joining NRC he was a post-doctoral fellow with C. Glinka (National Institute of Standards and Technology, USA) and S. Kumar (Pennsylvania state University, USA), and subsequently an NSERC visiting fellow with J. Katsaras. He received his PhD under the direction of D.A. Hoagland (University of Massachusetts) studying polymer chain conformation under elongational flow. He is interested in understanding the mechanisms of self-assembly in a variety of soft materials using small angle neutron scattering techniques.

John Katsaras

John Katsaras is an NRC Senior Research Officer and Science Group Leader. Prior to coming to NRC he was research associate with Atomic Energy of Canada Limited (Chalk River Laboratories, Canada). He received his PhD in Biophysics from the University of Guelph under the supervision of R.H. Stinson. His research interests focus on the understanding of model membranes in the context of biology, and their medical applications.

$E_f - E_i = h\omega$ is also reflected in the scattering function $S(\vec{q}, \omega)$. It should be pointed out that neutron scattering lengths do not only change from element-to-element, but can also differ between the element's isotopes (*e.g.*, hydrogen and deuterium), giving neutrons a great advantage in the study of soft materials inherently rich in hydrogen.

There is another advantage to scattering techniques. Although the quantum wave properties of any particle can be used for diffraction, using charged particles, as in the case of electron microscopy, often requires the sample to be placed in a complicated, evacuated sample environment. This is a less than ideal situation for soft and biological materials, where relevant *in situ* conditions (*e.g.*, hydration, pH) must be maintained. Among possible scattering probes such as X-rays and electrons, for the most part, only charge neutral neutrons lend themselves ideally to special sample containers that are easily fabricated, and whose temperature, hydration, shear forces and pressure are easily controlled.[2–6]

For many experiments, lipid dispersions or emulsions can be contained in thin walled glass or quartz capillary tubes (X-rays), or quartz cuvettes (neutrons), at the appropriate concentrations and temperature. Cuvettes for rheological studies can also be used. In some cases, such as thin films on a solid support, or Langmuir monolayers, orientational order can be imposed at 2D or 3D interfaces. In these cases, the sample container design can get rather complicated, where the position of the entrance and exit beams, relative to the sample interface, must be carefully considered (see Fig. 1), as we shall see for the various applications described below.

1.1 Production of neutrons and X-rays

1.1.1 Neutrons. Neutron beams with fluxes suitable for scattering experiments are produced either by nuclear reactors (*e.g.*, National Research Universal NRU, Chalk River, Canada), where the fission of uranium nuclei (^{235}U) results in neutrons with energies ranging between 0.5 and 3 MeV, or by spallation sources (*e.g.*, Spallation Neutron Source SNS, Oak Ridge, USA), where accelerated charged sub atomic particles strike a heavy metal target (*e.g.*, Hg, Ta), expelling neutrons from the target nuclei.

In order to produce neutrons suitable for the study of soft materials, so-called "fast" neutrons are slowed down, or "thermalized", by passing through and interacting with a moderator (*i.e.*, H_2O, D_2O, graphite, Be). Thermal neutrons can be further moderated when they pass through a cold moderator, for example liquid hydrogen (~20 K). These so-called "cold", lower energy neutrons can have wavelengths ranging from 5–20 Å, making them ideal probes for soft materials with inherent large unit cells.

1.1.2 X-Rays. X-Rays are commonly produced when high energy incident electrons collide with and displace a heavy metal target's (*e.g.*, Cu, Mo) *K*-shell electrons. When *L*- and *M*-shell electrons cascade down to fill the *K*-shell vacancies, the energy released results in the intense characteristic K_α and K_β X-rays—each target element has its own characteristic K_α and K_β X-rays.

Intense X-ray beams are produced by synchrotron radiation sources, large circular rings where charged particles, such as electrons or positrons are guided around the ring through a series of bending magnets at speeds approaching that of light in vacuum. As the magnets alter the electron's path, they are accelerated toward the centre of the ring emitting synchrotron radiation. The latest, so-called third generation synchrotrons (*e.g.*, Advanced Photon Source APS, Chicago, IL, Spring 8 Hyogo, Japan and the European Synchrotron Radiation Facility ESRF, Grenoble, France), are ~10^{10} times more brilliant (photons/s/mm^2/mrad^2) than first generation synchrotron sources and 10^{15} times more brilliant than conventional sealed tubes and rotating anodes. For more complete details regarding neutron and X-ray production, the reader is referred to a recent article by Katsaras *et al.*[7]

Unlike many techniques, scattering is not a probe of local structure. In every application of scattering the data will arise from an average of the sample bulk, determined by the size of the sample and the confined shape of the beam. With X-ray beams of suitably high intensity, beam size can vary between microns and millimetres, while typical neutron beams are considerably larger, upwards of a few centimetres. For the most part, large neutron beams are necessary, because of the much lower flux of neutrons compared to X-rays.

1.2 Applications in biotechnology and biophysics

Self assembled lipid nanoparticles are of great interest for a variety of potential applications. Perhaps their most important use is as mesoscale, biocompatible carriers of large biomolecules such as drugs, proteins and DNA. In addition, dispersions of naturally derived lipid surfactants find application in a number of colloid technologies, where condensed lipid assemblies may find use in the fabrication of one-, two- and three-dimensional nanomaterials. Scattering and diffraction have revealed much about the basic structure and thermotropic phase behavior in solution of these nanoparticles.[8]

The study of the biophysical properties of lipids is still very much an active area of research. Important basic structural parameters such as bending rigidity,[9] spontaneous curvature,[10] and lipid areas[11] and volumes[12] are routinely measured by scattering methods. Many of these types of experiments have been dealt with elsewhere *e.g.*[13–15] Here we focus on novel systems of lipid mixtures, and of biological and synthetic molecules where scattering techniques have been used to yield new information. For example, for a recent review of how scattering and diffraction have contributed to our understanding of how biocide polymers interact with cell membranes, see ref. 16.

2 Diffraction

Diffraction is built around the simple principle of Bragg's law, introduced in first year physics, for the reflection of waves from repeating objects. This idea is captured in the simple equation for a wave of wavelength λ reflecting from a series of planes of atoms at angle θ. Constructive interference will take place when the angle and the spacing between the planes of atoms, d, are related by

$$\lambda = 2d\sin(\theta) \quad (2)$$

where h is an integer that indicates the number of wavelengths difference between the constructively interfering waves.

In more detail, the location of scattering atoms $\vec{r}_i$ from equation 1 can be rewritten in terms of the atom layers representing a repeating structural unit. For example, if a one-dimensional fundamental structural motif has a repeating size d, then the total sample may have N repeating layers of this motif, for a total thickness of Nd. An atom located at position R_i in the first unit is repeated in all units, and it is found at the location within layer h at

$$r_i = hd + R_i \tag{3}$$

In this case, the sum of eqn 1 becomes

$$\sum_i f_i e^{i\vec{q}\cdot\vec{r}_i} = \sum_n f_n e^{i\vec{q}\cdot\vec{R}_i} \sum_h e^{ih\vec{q}\cdot\vec{d}} \tag{4}$$

where the first sum is over all atoms in just one structural motif. This term modulates the second sum which now takes in to account the total number of repeating units making up the sample. The second term can have a very strong maximum when $q\cdot d = h2\pi$, which translates in to Bragg's law when $|\vec{q}| = |\vec{k_f} - \vec{k_i}| = 4\pi\sin\theta/\lambda$. Therefore, structural motifs in lipid dispersions that repeat with well defined correlation lengths give rise to extremely strong constructive interference. At the very least, knowledge of the wavelength and scattering angle will reveal the measured d.

2.1 Small angle diffraction

It is the application of Bragg's law to peaks in the diffraction pattern that reveals the dimensions of strongly correlated structures, such as crystal planes, or smetic layers of membranes. Repeating structural units of lipid assemblies in liquid crystalline phases are ordered enough to provide pseudo Bragg diffraction of X-rays and neutrons. Diffraction from ordered solution samples is often called small angle diffraction (SAD), where the Bragg-like scattering reveals core structural dimensions by direct crystallographic means (*i.e.* Bragg's law).

2.1.1 Small angle diffraction: biotechnology. The use of diffraction in structure determination of solid lipid nanoparticles (SLNP) includes a long list of technological applications of lipid complexes.[17–20,8] Interesting highlights include natural lamellar vesicles incorporating glycolipid surfactants for possible use in cosmetics,[21] lipids to improve the solubility of flavour compounds dissolved in maize starch,[22] and lipid lamellar phases to control the alignment and growth of gold colloidal nanoparticles.[23]

Quantum dots are semiconductors whose small size confines their excitations in all dimensions, leading to unique spectroscopic properties. Dots made of CdSe/ZnS, for example, have been found to induce a transition of unilamellar vesicles in to a lamellar hybrid condensed phase, making the dots less biologically toxic.[24]

Diffraction can also reveal the core dimensions of a variety of unusual shaped lipid nanoparticles, such as lipid nanotubes formed by N-(11-cis-octadecanoyl)-β-D-glucopyranosylamin;[25] precipitates of cationic and anionic surfactant mixtures, such as tetradecyl-trimethyl-ammonium laurate;[26] and progesterone loaded "hexosomes", hexagonal nanoparticles made of monolein and oleic acid and surfactant.[27]

There have been many attempts at improving DNA transfection by rational design of transfection agents. A recent example is an X-ray SAD study of gemini surfactant based nanoparticles incorporated with DNA, whereby the nanoparticles form weakly ordered structures and multiple phases.[28,29] These phases correlate with the measured enhanced DNA transfection due to the addition of amines in the spacer of the gemini surfactant block. These chemical additions add to the potential of the agent to adopt complex morphologies, as measured by X-ray SAD, which in turn lead to better cell transfection.[29]

Small and wide angle diffraction are routinely used to monitor the effects of lipid crystallinity on the physical and chemical properties of additives for drug encapsulation, such as cetyl palmitate SLNP,[30] or goat fat modified beeswax.[31] SLNPs with high melting transitions exhibit gel-like polymorphism in their diffraction patterns that show how their crystallinity can protect the antioxidant, namely α-tocopherol, against oxidation, extending the life of such vitamin supplements.[32]

Novel designs of cationic polymeric liposomes appear frequently in the literature, such as those with unilamellar and multilamellar phases similar to dipalmitoyl phosphatidylcholine (DPPC), where both hydrophobic (*e.g.*, oil soluble magnetic nanoparticles) and hydrophillic molecules can be independently solubilized in its matrix.[33] For more complex crystallinity, kinematic scattering theory has been applied to the small angle X-ray diffraction patterns of crystalline triglyceride nanoparticles in dispersion—a system with considerable complexity and many unusual features in its scattering curves.[34]

An interesting observation of cell microstructure is in the case of molecular confinement. It is possible to mimic such confinement by passing biomolecules, such as lipids, through patterned microfluid channels, and using micro X-ray diffraction to examine how order arises at different points in the channel.[35]

2.1.2 Small angle diffraction: biophysics. In addition to phase characterization, the change in diffraction maxima can signal important alterations to membrane structure, which in turn may have profound biological implications. For example, many pharmaceutical agents, such as antipsychotic drugs, may exert their effects directly on lipid structure and organization.[36] Barbaloin (hydroxyanthraquinone), is an extract of aloe found in foods and cosmetics, and it incorporates into negatively charged DMPG bilayers at low and high ionic strength such that it increases the packing of the hydrocarbon chains.[37] This result suggests a mechanism for the health claims of barbaloin, namely that it reduces inflammation and infection by altering membrane bound receptors of inflammatory signaling molecules through changes in the membrane itself.

The basic physical chemistry of nonlamellar forming lipids has long been a topic of interest. Recent theories of membrane curvature energy have been tested by diffraction,[38,39] and a review of biological based chemical sensors modeled on membrane proteins and bicontinuous lipid cubic phases explains how diffraction can elucidate their structure.[40] An interesting

example of this comes from exploring how confinement in lipid cubic mesophases can affect the aggregation and amyloid formation of proteins such as insulin, which hints that troublesome storage of aggregating proteins may be overcome by non-lamellar lipid phases.[41] A recent review of how lipid structure can influence protein function, and *vice versa*, explores how much of this evidence comes from diffraction techniques.[42,43]

2.2 Lamellar diffraction

Diffraction from ordered samples on a substrate or a flat interface is another example of a diffraction application of biologically relevant systems. Historically, liquid crystal diffraction has been used to determine the near atomic structure of the one-dimensional lipid bilayer profile perpendicular to its surface. This is done through standard Fourier reconstruction of the diffraction pattern to calculate either an electron density map, in the case of X-rays, or a scattering length density profile, in the case of neutrons.

Through deuterium labeling, neutron diffraction can determine the distribution of water or of individual components. The ability to isolate individual molecular groups at atomic level of detail is unique among biophysical techniques, as it does not require model fitting or other interpretation of the data. Furthermore, discovery of the center of mass distribution of a chemical group is information directly comparable to molecular model simulations without the need for additional computations.

An example of this type of experiment is shown in Fig. 2 for the case of cholesterol's reorientation in polyunsaturated lipids.[44] The multiple roles that cholesterol plays in membrane organization has for decades been a topic of intense experimentation. Coupled with the emergence of polyunsaturated fatty acids (PUFA) as an important dietary supplement, it has become evident of how important it is to understand how these two lipids interact. Various microscopic techniques reveal the domain organizing effects of cholesterol in membranes, but cannot peer deeply into their molecular interactions. For example, NMR (Nuclear Magnetic Resonance) reveals significant motional constraints of cholesterol in PUFA environments, but cannot on its own formulate any molecular picture. Only diffraction can directly probe the molecular interactions and alterations to lipid structure.

On the left of Fig. 2 is an example of diffraction data measured from stacks of lipid lamellae aligned on a solid substrate (a single crystal of silicon) and hydrated in a controlled humidity atmosphere. The Bragg peaks at regular intervals of the scattering vector $\vec{q}$ are the amplitudes of the sum found in eqn 4, for $h = 1$, 2, 3…. Since $\vec{q}$ is determined by the incident beam and the angle of detection in the laboratory frame of reference, the orientation of the aligned sample maintains the condition of $\vec{q} \parallel \vec{r}$, as shown in the middle of Fig. 2. The inverse Fourier transform of eqn 4 then corresponds to the scattering strength in the $\vec{r}$ direction, which peaks around chemical groups with associated deuterium atoms, and dips in regions with more hydrogen atoms. In the subtraction of two experiments whose difference is only the substitution of deuterium atoms, all native components should subtract away, leaving only the distribution of deuterium, as shown on the right hand side of Fig. 2.

Fig. 2 reveals that the deuterium label at the head group is unexpectedly located at the center of the lipid bilayer, contrary to its textbook "upright" orientation. This result explains the motion constraints seen by NMR, and its rapid movement across the bilayer with the higher disorder and permeability as found in PUFA[45] and short monounsaturated lipid[46] simulations. In addition, it provides justification for models of cholesterol solubilization in various lipids species that predict greatly reduced affinity between PUFA and cholesterol. In this case, the lowest energy location for cholesterol is in the terminal methyls of the PUFA lipids.

Such deuterium labeling is becoming more popular and for example, has revealed insights into protein folding mechanisms[47] and the physical properties of membranes after the incorporation of inclusions, such as cucumin spice[48] and plant sterols.[49] Amphiphilic block copolymers, such as $PEO_nPPO_mPEO_n$, are often used to modify cell membrane structure and function. One-dimensional electron density maps derived from synchrotron X-ray scattering show that the PPO unit is the critical determining factor in the association and incorporation of the polymer into lipid bilayers.[50]

Better determination of the membrane's structural properties then allows for better understanding of biological properties, and

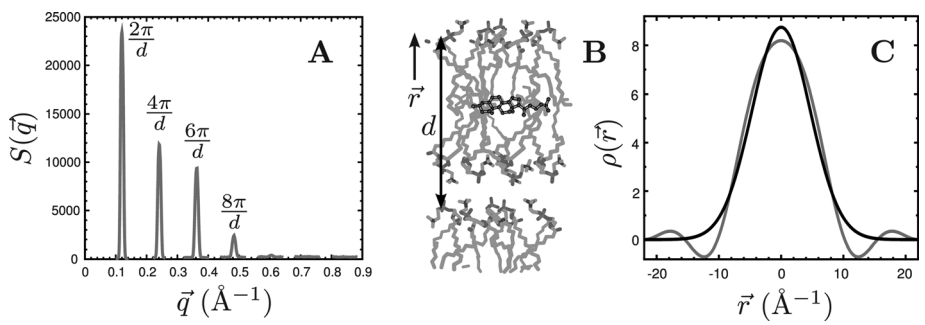

Fig. 2 An example of lamellar diffraction. Data adapted from ref. 44. A. Raw data of the neutron diffraction from aligned stacks of lipid and water, with 10 mol% cholesterol, as shown in B. Bragg peaks appear at integer multiples of 2π divided by the lamellar spacing, d. The amplitude of these peaks are used in the Fourier reconstruction of the scattering length density in a direction perpendicular to the plane of the bilayer. C. By using cholesterol with and without deuterium label (in this case, near the 3β-hydroxyl group), subtraction of the two bilayer profiles reveals the mass distribution of the label with nanometre resolution. In this example, cholesterol was surprisingly found to reside at the center of PUFA bilayers, rather than in its normal "upright" position.

the association between membrane structure and its function. For example, enhanced biological activity of Na^+-lipopolysaccharide (LPS) bacterial membrane isolated from *Pseudomonas aeruginosa* PAO1 was correlated with increased levels of hydration, where a significant amount of water was found to penetrate deep into an LPS bilayer, including the bilayer hydrophobic center.[51] Subsequently, Kučerka *et al.*,[52] using one-dimensional neutron scattering length density profiles, showed that water penetrates Ca^{2+} LPS bilayers to a lesser extent than either Na^+ and Mg^{2+} bilayers. This differential water penetration could have implications as to how small molecules permeate the outer membrane of Gram-negative bacteria, and possibly, how non-lamellar phases are formed.

Recent experiments show that omega fatty acid lipid bilayers are measurably thinner in the hydrocarbon region compared to standard egg PC lecithin,[53] which has implications for how the function of G-protein coupled membrane receptors might be regulated by the membrane.[54] In fact, membrane protein structure, and thus its function, has long been thought to be controlled in large part by its membrane environment. To that end, lamellar diffraction has recently revealed the first highly detailed, physiologically relevant electron density profile of the alamethicin induced transmembrane pore.[55] Such data can be used as test beds for ion channel theories.

The natural lamellae of the stratum corneum (SC) have lent themselves directly to investigation by lamellar diffraction. In the case of recent examples, it has been found that increasing the chain length of the free fatty acid in an SC model membrane (made from ceremide lipids) induces the fatty acid into forming a partially interdigitated phase.[56] Complementary neutron diffraction revealed the arrangement of the ceremide molecule in the SC membrane.[57,58]

2.3 Grazing incidence diffraction

Self assembly in two-dimensions is easily attained by lipids and insoluble proteins at the air–water interface, such as for example, with Langmuir films. Grazing incidence diffraction (GID) is often used to detect any ordering in the 2D plane, as lamellar diffraction does along the 1D direction perpendicular to the membrane.

In GID, the beam's angle of incidence to the sample plane, $\vec{k}_i$, is below the critical angle of total reflection. The detector is scanned over many different directions $\vec{k}_f$, such that the momentum vector $\vec{q} = \vec{k}_f - \vec{k}_i$ is recorded over many length scales in directions perpendicular ($\vec{q}_\perp$) and parallel ($\vec{q}_{||}$) to the water surface. In this way, several types of information can be obtained. Langmuir monolayers are 2D assemblies of molecules azimuthally randomly oriented on the water surface. Data in the $\vec{q}_{||}$ direction will give intense Bragg peaks at $d = 2\pi/q_{||}$, where d is the intermolecular distance of the 2D lattice structure. If the long axis of the molecule, for example the linear hydrocarbon tails of lipids, are tilted with respect to the water surface, then Bragg diffraction occurs at values of $\vec{q}_{||}, \vec{q}_\perp$, which gives information on the direction and magnitude of molecular tilt, the surface roughness and perhaps even the coherence length of the crystalline domains.

The 2D crystallization in a lipid monolayer, such as that achieved by cholera toxin bound to its ganglioside receptor,[59] may be the only way to determine the structure of membrane bound proteins that are difficult to form into 3D crystals. Self assembled polymers, conjugated with β-sheet forming peptides have also been studied at the air–water interface with GID.[60] In an effort to understand the toxicology of nonsteroidal anti-inflammatory drugs, their interaction with lipid membranes was studied by X-ray GID and SAD, and shown to have profound perturbation effects on membrane integrity.[61]

3 Small angle scattering

Whereas diffraction often focuses on atomic properties and dimensions, small angle scattering (SAS) deals with assemblies of molecules whose length scales are of the order of tens of nanometres and microns, in which case it is easier to think in terms of bulk material properties. Small angle scattering differs from diffraction in that although there is a measurable amount of structural correlation, there is no crystalline-like ordering. In this case, a dilute assembly of identical and randomly oriented scattering objects gives rise to correlations that can reveal the morphology of a sample without crystalline order. For SAS, the strength of the interaction between probe and atom is averaged over some volume V containing the atoms:

$$\rho(\vec{r}) = \frac{1}{V}\sum_i f_i \tag{5}$$

For X-rays, ρ is the electron density, and for neutrons, it is the scattering length density. Now the discrete sum of eqn 1 becomes an integral over the sample volume

$$S(\vec{q}) = \frac{1}{V}\left|\int_V \rho(\vec{r}) e^{i\vec{q}\cdot\vec{r}} \mathrm{d}^3\vec{r}\right|^2 \tag{6}$$

The integral in eqn 6 can be broken down into two parts

$$S(\vec{q}) = \frac{1}{V}\left|\int_{V_1} \rho(\vec{R}) e^{i\vec{q}\cdot\vec{R}} \mathrm{d}^3\vec{R}\right|^2 \left|\sum_i e^{i\vec{q}\cdot\vec{r}_i}\right|^2 \tag{7}$$

where the first integral is known as the form factor—the scattering produced by the prototypical scattering of a single macromolecular assembly, while the second term is a sum describing the discrete spatial correlations of the assemblies in solution.

Interpreting SAS data often requires some idea of the shape of the mesophase, $\rho(\vec{r})$, and an iterative fitting of the measured data to extract detailed morphological shapes and dimensions. However, clues to the dimensionality of the morphological structures can be found through the application of scattering approximations to various parts of $\vec{q}$. For example, the principle of Porod analysis is that for $\vec{q}$ values at the high end of the small angle regime, the scattered intensity scales as $\propto S/q^4$, where S is the surface area of the macromolecular objects in solution. Guinier analysis, on the other hand, holds that for smaller $\vec{q}$ values, the scattered intensity scales as $\propto exp(-R_G^2 q^2)$ where R_G is the object's radius of gyration—it should be noted that the concept of the radius of gyration is only applicable to dilute systems.

3.1 Small angle scattering: biophysics

The two prototypical samples in biophysics whose large and uniform size in solution have lent themselves to study by SAS are viruses and spherical lipid vesicles. In the latter case, theories of how other molecules can interact with these cell mimics can be tested in dilute, but tightly controlled solution conditions. Here we outline some interesting recent examples.

Prototypical SAS data from lipid unilamellar vesicles is shown in Fig. 3. On the right is a schematic of such a vesicle with its primary dimensions shown. Vesicles can be loaded or decorated by other molecules, such as payloads of drugs or DNA, either contained within the hydrophillic solvent interior, or bound to the hydrophobic lipid shell. On the left side of Fig. 3 is data from SAS of dilute solutions of these vesicles, for both X-rays and neutrons. For these experiments, X-ray data provided valuable information regarding the bilayer's detailed structure, while water distribution and gross bilayer morphology was best determined by neutrons. The advantage of the neutron data becomes obvious as the three data sets are from essentially the same system with deuterium either in the solvent, in the form of ^2H_2O (heavy water), or deuterium replacement on the lipid acyl chains. In total, the four data sets represent four independent aspects of scattering contrast enhancing the contribution to the scattering from various parts of the system, such as lipid headgroups, chains, or solvent. All four data sets can then be simultaneously fit to a single structural model, greatly increasing the available information, thus reducing the degrees of freedom and lowering the uncertainty of the various structural parameters. The data shown in Fig. 3 were recently used to determine the area per lipid of fully hydrated 18:0-18:0 PC lipid with great accuracy.[11]

Spontaneously forming small unilamellar vesicles (SULVs) are easy to prepare and show great promise for use in delivering therapeutic payloads. SULVs made up of the ternary phospholipid mixture, dimyristoyl-phosphatidylcholine (DMPC), dihexanoyl-phosphatidylcholine (DHPC) and dimyristoyl-phosphatidylglycerol (DMPG) have been characterized by small angle neutron scattering (SANS).[62] These low polydispersity (0.14–0.19) SULVs range in size (*i.e.*, radius) from 110 to 215 Å and are capable of entrapping, and subsequently releasing hydrophilic molecules (*e.g.*, fluorescent dyes and quenchers) in a controlled fashion. Compared to SULVs produced by traditional methods (*e.g.*, sonication or extrusion), spontaneously forming SULVs are unique in that they lend themselves ideally to industrial production as they are easy to prepare in large quantities. Presently, other components (*e.g.*, cholesterol, PEGylated lipids and antibodies) have been incorporated into the system in order to produce more impermeable, targeted and stealth-like SULVs. Cationic, anionic and zwitterionic liposomes have also been used as vectors of the cancer drug octa(carboranyl)porphyrazine. In this case, SAS was employed to find the best loading method and conditions for stability and drug density.[63]

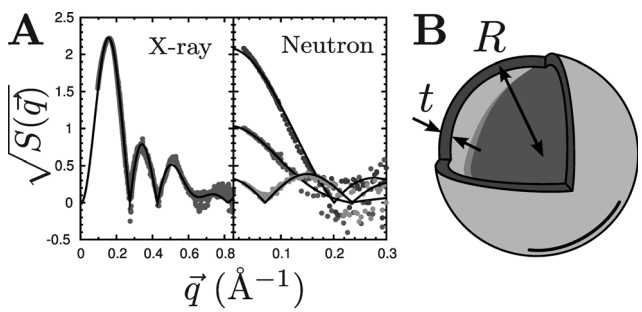

Fig. 3 An example of small angle scattering. Data adapted from ref. 11. A. Essentially identical phospholipid vesicles in solution were prepared by extrusion, and examined by X-ray and neutron SAS. With neutrons, the data were taken in 50% and 100% D_2O, and the acyl chains have varying degrees of deuterium labeling. In this way, the independent data sets can be fitted simultaneously to the same model of eqn 7, (shown as black lines) whose parameters include the vesicle radius and the bilayer thickness, as shown in B. Kučerka *et al.* were able to use the extra information provided by the additional neutron contrast variation to better determine phospholipid structural parameters, including per lipid area and volume.

Monitoring changes of structural parameters may reveal biophysical modes of actions of other molecules. For example, the Alzheimer's peptide Aβ(142) was discovered to have vesicle fusion activity as seen through the increase in vesicle radius with Aβ oligomer concentration (but not with amyloid aged Aβ).[64] Such activity may have not been noticed by other experimental methods, and the result adds gravity to the theory that oligomers formed by Aβ on their way to folding into amyloid fibrils are cytotoxic by attacking cell membranes.

Producing high quality crystals of membrane bound proteins has proven to be very difficult. However, lipid mimetic alkyl monoglucoside micelles combined with PEG can be used in protein crystallization schemes. Neutron SAS has shown that PEG alters the strength and range of intermicellar interactions, but has minimal impact on the geometry of the micelles.[65] Knowledge of the micelle size and aggregation tendencies is key to choosing the optimal membrane protein crystallization conditions.

3.2 Small angle scattering: biotechnology

The size and shape of several novel dilute lipid nanoparticles have been characterized by SAS. It has long been a goal to fill the hollow core of most vesicles with payloads that can then be delivered to a region of interest within patients. For example, "magneto vesicles" are lipid vesicles containing magnetic nanoparticles in their structure, which are interesting because the magnetic components of the vesicles allow for guided portation by an external magnetic field. The only technique that allows for the *in situ* direct measurement of their size and structure is small angle neutron scattering with contrast enhancement by heavy water. In a recent study, Chen has shown that magneto vesicles prepared by extrusion of lipid dioleoyl-phosphatidylcholine (DOPC) and citrate coated magnetic nanoparticles (Fe_3O_4) in solution, retain the structural characteristics of their basic constituents. This means that such particles have the same suitability for medical applications as pure DOPC liposomes.[66]

Structural parameters of such lipid nanoparticles can be measured with considerable accuracy. For example, phospholipid and chitosan, a cationic polysaccharide, form nanoparticles with the ability to carry and deliver the cancer drug tamoxifen citrate within the hollow core of multilamellar spheres of radius

~440 Å.[67] Liposils are silica based ceramic capsules patterned over a lipid vesicle substrate, and X-ray SAS revealed a shell thickness of ~5.5 nm.[68]

Nanodiscs are discoidal particles consisting of artificial amphipathic proteins that wrap themselves around the circumference of a lipid bilayer in a belt-like manner, after the whole system is assembled by the introduction of cholate. The stoichiometry of the nanodiscs were determined through their SAXS determined dimensions.[69] Discoidal particles were also proposed as the phase of triglycerides in the liquid state,[70] a phase for which surprisingly very little was known. Morphologies very different than spherical vesicles are also to be expected, although their usefulness in technological applications is not obvious. For example, surfactant-lipid-sterol systems form unusually thick helical ribbons, despite the absence of a bilayer structure and the predominance of sterol in their composition.[71]

4 Reflectometry

In the discussion of scattering and diffraction, we were implicitly working within the Born approximation by assuming that neutrons and X-rays are scattered only once on passing through the sample. In that weak scattering approximation, we can assume that the total scattering can be calculated by assuming the scattering arises from each atom in the sample, as shown in eqn 1. The reflection of waves from surfaces is however, quite different since at very low angles of incidence the wave is capable of total external reflection, which is certainly not weak scattering.

The reflection of waves at interfaces is adequately described by Fresnel's equations, one result of which is the familiar Snell's law of refraction due to waves passing through two media having different indices of refraction. The role of the index of refraction for light is generally familiar, but perhaps not for neutrons and X-rays.

Reflectivity is simply the fraction of photons or neutrons elastically reflected from a surface from the total number incident on the sample. When measured as a function of $\vec{q} = \vec{k_f} - \vec{k_i}$, where $\vec{k_f}$ and $\vec{k_i}$ make equal angles to the surface, the reflectivity curve contains information regarding the profile of the sample in the direction normal to its surface. Constructive interference from multiple surfaces (interfaces) yield the thickness of the film and any sublayers. If one knows the chemical composition of the film, the concentration of a particular chemical species at a given depth in the film can be determined.

Reflectometry of single supported membranes has also been used to measure the physical properties of fluctuating membranes. Similar to pipette aspiration, a single bilayer can be probed, but in a flat geometry in the absence of curvature. Similar to multilamellar stacks, confinement effects can be studied, but with a single surface of either a hard crystalline substrate or a cushioned polymer base.[72,73]

The most wide application of reflectivity to lipid structure is the investigation of the interaction of various compounds and proteins with lipid membranes. Generally, these studies have fallen into two types: solid supported or tethered bilayers, and liquid/air mononolayers. In both cases, various solution parameters such as temperature, ionic strength and molecular concentration can be controlled *in situ*. An advantage of spreading monolayers at the air–water interface is the ability to also control *in situ* the lateral packing pressure of the lipids.

A simple example of reflectometry data is shown in Fig. 4.[74] It is commonly found that artificial hard surfaces present a location for protein aggregation *in vivo* or in test equipment exposed to biological fluids. It is hoped that custom designed surface coatings that are made from more biologically compatible materials will prevent this "biofouling". Such thin films may only be nanometres thick, and measuring their structural dimensions to see if the method of manufacture results in the desired surface with the preferred properties, is difficult. Ellipsometry data is often inconclusive without knowledge of the dielectric constant of the material. Furthermore, while attenuated total reflection infrared spectroscopy may be very sensitive to *changes* in surface structures, determination of a static surface structure requires interpretation of the FTIR (Fourier transform infrared spectroscopy) absorption bands.

In the lower part of Fig. 4, we see a possible anti biofouling surface coating, namely PEG-methacrylate grafted on to the surface of a silicon crystal. The upper part of the figure shows

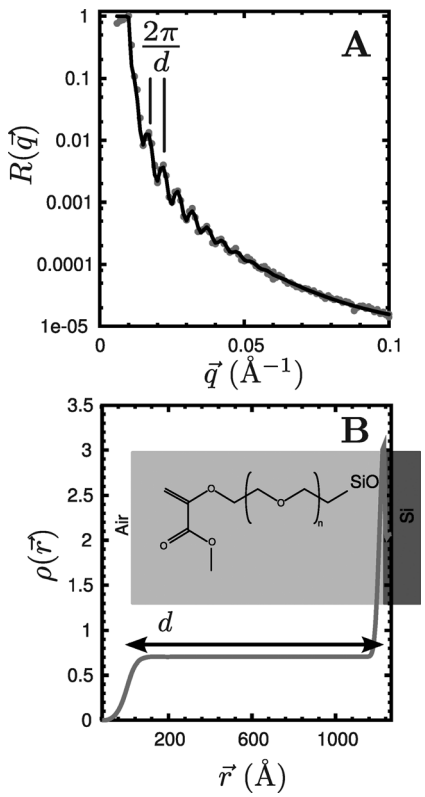

Fig. 4 An example of neutron reflectivity data adapted from ref. 74. A. The reflected intensity $R(\vec{q})$ for a thin film as a function of $\vec{q}$ (for X-rays and neutrons), falls off as $\sim q^{-4}$. Interference fringes occur because of multiple reflections between more than one interface of material, in this case, between air and a layer of biocompatible PEG-methacrylate grafted to the surface of a silicon crystal. The iterative fitting to the data (black line) involves the construction of a model profile of the thin film, shown in B. In this experiment, the same sample was exposed to bulk water and the water–film interface was monitored for changes upon the addition of proteins into solution in hopes that the polymer would resist aggregation and biofouling by the protein.

both the total reflection of neutrons from the surface at very low q, as well as the q^{-4} drop off of reflected intensity, as predicted by Fresnels' equations. The two dominant interfaces present in the sample, the polymer–air and polymer–substrate, give rise to multiple interference reflections, which manifest themselves as oscillations in $R(\vec{q})$ and are directly related to the overall polymer layer thickness. This sample was then tested in solution, under different temperatures and ionic strengths, and it was determined that the density of polymer grafted to the surface was very much in line with what was predicted from the experimental protocol.[74]

Several proteins have been tested for their ability to penetrate the lipid environment by reflectivity. This has led to some interesting discoveries, such as a critical lateral pressure for the insertion of a transcription activating factor derived peptide[75]—a peptide which acts as an agent capable of ferrying cargo across cell membranes. Another study of membrane adsorbed peptide structure utilized partially folded α helix motifs that interacted with lipid monolayers through divalent metal ion-histidine interactions. The number and placement of the histidine were seen to control the thickness of the absorbed layer (within ± 2.5 Å), as well as the orientation of the peptide. The chain order was also monitored simultaneously by X-ray GID.[76]

Continuing focus on the possible cell toxicity of Alzheimer's peptide includes reflectivity experiments, since simple membrane mimics are easy to prepare. The type of Aβ association with lipid monolayers was found to depend on lipid composition and subphase condition, with negatively charged lipids having the ability to induce Aβ fibrillogenesis.[77]

5 Conclusions

Diffraction, scattering and reflectometry have become indispensable tools for the identification of lipid phases and measurement of their structural dimensions. In this brief review, we have highlighted the main scattering techniques employed in soft materials research. Lamellar ordering can be easily used to identify the length scales of the ordered system by diffraction, and with sufficient pseudo crystalline order. Even crystallographic techniques can be used to determine structure on the nanometre scale. In the absence of order, small angle scattering can be employed, and with judicious use of contrast enhancement, it can identify the shapes and sizes of mesophases present in most lipid nanoparticles. Finally, lipids at surfaces can be studied by reflectometry and grazing incidence diffraction. We have illustrated each technique with some papers that have used scattering or diffraction as a matter of course in the last couple of years. These experiments cover a range of disciplines, from pure biophysics to applications of biotechnology affecting our daily lives.

References

1 T. A. Harroun, G. D. Wignall, and J. Katsaras, in *Neutron Scattering in Biology: Techniques and Applications (Biological and Medical Physics, Biomedical Engineering)*, ed. J. Fitter, T. Gutberlet, and J. Katsaras, Springer, Heidelberg, Germany, 1st edn, 2006, ch. 1, pp. 1–18.
2 J. Katsaras, *Biophys. J.*, 1997, **73**, 2924–2929.
3 J. Katsaras, *Biophys. J.*, 1998, **75**, 2157–2162.
4 M. J. Watson, M. P. Nieh, T. A. Harroun and J. Katsaras, *Rev. Sci. Instrum.*, 2003, **74**, 2778–2781.
5 T. A. Harroun, F. Fritzsche, M. J. Watson, K. G. Yager, O. M. Tanchak, C. J. Barrett and J. Katsaras, *Rev. Sci. Instrum.*, 2005, **76**, 065101.
6 J. Katsaras, T. A. Harroun, M. P. Nieh, M. Chakrapani, M. J. Watson, and V. A. Raghunathan, in *Neutron Scattering in Biology: Techniques and Applications (Biological and Medical Physics, Biomedical Engineering)*, ed. J. Fitter, T. Gutberlet, and J. Katsaras, Springer, Heidelberg, Germany, 1st edn, 2006, ch. 7, pp. 107–126.
7 J. Katsaras, J. Pencer, M. P. Nieh, T. Abraham, N. Kučerka, and T. A. Harroun, in *Structure and Dynamics of Membranous Interfaces*, ed. K. Nag, Wiley, Hoboken, New Jersey, 1st edn, 2008, ch. 5, pp. 107–134.
8 H. Bunjes and T. Unruh, *Adv. Drug Delivery Rev.*, 2007, **59**(6), 379–402.
9 S. H. Alley, O. Ces, M. Barahona and R. H. Templer, *Chem. Phys. Lipids*, 2008, **154**(1), 64–67.
10 H. Seto, M. Hishida, H. Nobutou, N. L. Yamada, M. Nagao and T. Takeda, *J. Phys. Soc. Jpn.*, 2007, **76**(5), 054602.
11 N. Kučerka, J. F. Nagle, J. N. Sachs, S. E. Feller, J. Pencer, A. Jackson and J. Katsaras, *Biophys. J.*, 2008, **95**(5), 2356–2367.
12 N. Kučerka, S. Tristram-Nagle and J. Nagle, *J. Membr. Biol.*, 2006, **208**(3), 193–202.
13 J. Katsaras and T. Gutberlet *Lipid Bilayers: Structure and Function, Biological Physics Series*, Springer, 2000.
14 J. F. Nagle and S. Tristram-Nagle, *Biochim. Biophys. Acta*, 2000, **1469**, 159–195.
15 N. Kučerka, M. P. Nieh, J. Pencer, T. Harroun and J. Katsaras, *Curr. Opin. Colloid Interface Sci.*, 2007, **12**(1), 17–22.
16 G. J. Gabriel, A. Som, A. E. Madkour, T. Eren and G. N. Tew, *Mater. Sci. Eng., R*, 2007, **57**(1–6), 28–64.
17 S. Kamiya, M. Yamada, T. Kurita, A. Miyagishima, M. Arakawa and T. Sonobe, *Int. J. Pharm.*, 2008, **354**(1–2), 242–247.
18 G. Caracciolo, D. Pozzi, R. Caminiti, C. Marchini, M. Montani and H. Amenitsch, *J. Appl. Phys.*, 2008, **104**(1), 014701.
19 G. A. Castro, L. A. M. Ferreira, R. L. Orefice and V. T. L. Buono, *Powder Diffr.*, 2008, **23**(2), S30–S35.
20 B. Yuan, L. L. Xing, Y. D. Zhang, Y. Lu, Z. H. Mai and M. Li, *J. Am. Chem. Soc.*, 2007, **129**(37), 11332.
21 W. Worakitkanchanakul, T. Imura, T. Fukuoka, T. Morita, H. Sakai, M. Abe, R. Rujiravanit, S. Chavadej, H. Minamikawa and D. Kitamoto, *Colloids Surf., B*, 2008, **65**(1), 106.
22 O. Tapanapunnitikul, S. Caiseri, D. G. Peterson and D. B. Thompson, *J. Agric. Food Chem.*, 2008, **56**(1), 220–226.
23 M. E. Meyre, M. Treguer-Delapierre and C. Faure, *Langmuir*, 2008, **24**(9), 4421–4425.
24 A. Dif, E. Henry, F. Artzner, M. Baudy-Floc'h, M. Schmutz, M. Dahan and V. Marchi-Artzner, *J. Am. Chem. Soc.*, 2008, **130**(26), 8289–8296.
25 H. Yui, H. Minamikawa, R. Danev, K. Nagayama, S. Kamiya and T. Shimizu, *Langmuir*, 2008, **24**, 709–713.
26 Y. Shen, J. Hao, H. Hoffmann and Z. Wu, *Soft Matter*, 2008, **4**(4), 805–810.
27 N. K. Swarnakar, V. Jain, V. Dubey, D. Mishra and N. K. Jain, *Pharm. Res.*, 2007, **24**(12), 2223–2230.
28 D. Uhríková, I. Zajac, M. Dubničková, M. Pisarčík, S. S. Funari, G. Rapp and P. Balgavý, *Colloids Surf., B*, 2005, **42**(1), 59–68.
29 S. D. Wettig, I. Badea, M. Donkuru, R. E. Verrall and M. Foldvari, *J. Gene Med.*, 2007, **9**(8), 649–658.
30 U. Ruktanonchai, S. Limpakdee, S. Meejoo, U. Sakulkhu, N. Bunyapraphatsara, V. Junyaprasert and S. Puttipipatkhachorn, *Nanotechnology*, 2008, **19**(9), 095701.
31 A. A. Attama and C. C. Mueller-Goymann, *Colloids Surf., A*, 2008, **315**(1–3), 189–195.
32 P. Relkin, J. M. Yung, D. Kalnin and M. Ollivon, *Food Biophys.*, 2008, **3**(2), 163–168.
33 X. F. Liang, H. J. Wang, H. Luo, H. Tian, B. B. Zhang, L. J. Hao, J. I. Teng and J. Chang, *Langmuir*, 2008, **24**(14), 7147–7153.
34 T. Unruh, *J. Appl. Crystallogr.*, 2007, **40**(6), 1008–1018.
35 H. M. Evans, R. Dootz, S. Koester, B. Struth and T. Pfohl, *Bull. Pol. Acad. Sci.*, 2007, **55**(2), 217–227.
36 C. Tessier, P. Nuss, G. Staneva and C. Wolf, *J. Colloid Interface Sci.*, 2008, **320**(2), 469–475.
37 E. Duarte, T. Oliveira, D. Alves, V. Micol and M. Lamy, *Langmuir*, 2008, **24**(8), 4041–4049.

38 D. P. Siegel and B. G. Tenchov, *Biophys. J.*, 2008, **94**(10), 3987–3995.
39 C. E. Conn, O. Ces, A. M. Squires, X. Mulet, R. Winter, S. M. Finet, R. H. Templer and J. M. Seddon, *Langmuir*, 2008, **24**(6), 2331–2340.
40 E. Nazaruk, R. Bilewicz, G. Lindblom and B. Lindholm-Sethson, *Anal. Bioanal. Chem.*, 2008, **391**(5), 1569–1578.
41 J. Kraineva, V. Smirnovas and R. Winter, *Langmuir*, 2007, **23**(13), 7118–7126.
42 D. Marsh, *Biochim. Biophys. Acta*, 2008, **1778**(7–8), 1545–1575.
43 D. Marsh, *Biophys. J.*, 2007, **93**(11), 3884–3899.
44 T. A. Harroun, J. Katsaras and S. R. Wassall, *Biochemistry*, 2008, **47**(27), 7090–7096.
45 S. J. Marrink, A. H. de Vries, T. A. Harroun, J. Katsaras and S. R. Wassall, *J. Am. Chem. Soc.*, 2008, **130**(1), 10–11.
46 N. Kučerka, J. D. Perlmutter, J. Pan, S. Tristram-Nagle, J. Katsaras and J. N. Sachs, *Biophys. J.*, 2008, **95**(6), 2792–2805.
47 X. Han, K. Hristova and W. C. Wimley, *Biophys. J.*, 2008, **94**(2), 492–505.
48 W.-C. Hung, F. Y. Chen, C.-C. Lee, Y. Sun, M.-T. Lee and H. W. Huang, *Biophys. J.*, 2008, **94**(11), 4331–4338.
49 A. Hodzic, M. Rappolt, H. Amenitsch, P. Laggner and G. Pabst, *Biophys. J.*, 2008, **94**(10), 3935–3944.
50 B. Lee and M. A. Firestone, *Biomacromolecules*, 2008, **9**(6), 1541.
51 T. Abraham, S. Schooling, M. P. Nieh, N. Kučerka, T. Beveridge and J. Katsaras, *J. Phys. Chem. B*, 2007, **111**(10), 2477–2483.
52 N. Kučerka, E. Papp-Szabo, M. P. Nieh, T. A. Harroun, S. R. Schooling, J. Pencer, E. A. Nicholson, T. J. Beveridge and J. Katsaras, *J. Phys. Chem. B*, 2008, **112**(27), 8057–8062.
53 K. Rajamoorthi, H. Petrache, T. McIntosh and M. Brown, *J. Am. Chem. Soc.*, 2005, **127**(5), 1576–1588.
54 K. Gawrisch and O. Soubias, *Chem. Phys. Lipids*, 2008, **153**(1), 64–75.
55 S. Qian, W. Wang, L. Yang and H. W. Huang, *Biophys. J.*, 2008, **94**(9), 3512–3522.
56 A. Ruettinger, M. A. Kiselev, T. Hauss, S. Dante, A. M. Balagurov and R. H. H. Neubert, *Eur. Biophys. J.*, 2008, **37**(6), 759–771.
57 D. Kessner, M. Kiselev, S. Dante, T. Hauss, P. Lersch, S. Wartewig and R. H. H. Neubert, *Eur. Biophys. J.*, 2008, **37**(6), 989–999.
58 D. Kessner, M. A. Kiselev, T. Hauss, S. Dante, S. Wartewig and R. H. H. Neubert, *Eur. Biophys. J.*, 2008, **37**(6), 1051–1057.
59 C. E. Miller, J. Majewski, E. B. Watkins, M. Weygand and T. L. Kuhl, *Biophys. J.*, 2008, **95**(2), 641–647.
60 A. Muenter, J. Hentschel, H. Borner and G. Brezesinski, *Langmuir*, 2008, **24**(7), 3306–3316.
61 M. Lúcio, F. Bringezu, S. Reis, J. L. F. C. Lima and G. Brezesinski, *Langmuir*, 2008, **24**(8), 4132–4139.
62 M.-P. Nieh, X. Qi and J. Katsaras, *Biochim. Biophys. Acta, Biomembr.*, 2008, **1778**, 1467–1471.
63 A. Salvati, S. Ristori, J. Oberdisse, O. Spalla, G. Ricciardi, D. Pietrangeli, M. Giustini and G. Martini, *J. Phys. Chem. B*, 2007, **111**(35), 10357–10364.
64 S. Dante, T. Hauss, A. Brandt and N. A. Dencher, *J. Mol. Biol.*, 2008, **376**(2), 393–404.
65 M. Santonicola, M. Yocum, A. Lenhoff and E. Kaler, *Langmuir*, 2007, **23**(10), 5358–5366.
66 K. Chen, *J. Dispersion Sci. Technol.*, 2007, **28**(6), 932–936.
67 Y. Gerelli, M. T. Di Bari, A. Deriu, L. Cantu, P. Colombo, C. Como, S. Motta, F. Sonvico and R. May, *J. Phys.*, 2008, **20**, 104211.
68 Y. Steinberg, A. Schroeder, Y. Talmon, J. Schmidt, R. Khalfin, Y. Cohen, J. M. Devoisselle, S. Begu and D. Avnir, *Langmuir*, 2007, **23**(24), 12024–12031.
69 A. Y. Shih, P. L. Freddolino, S. G. Sligar and K. Schulten, *Nano Lett.*, 2007, **7**(6), 1692–1696.
70 R. Corkery, D. Rousseau, P. Smith, D. Pink and C. Hanna, *Langmuir*, 2007, **23**(13), 7241–7246.
71 B. Khaykovich, C. Hossain, J. J. McManus, A. Lomakin, D. E. Moncton and G. B. Benedek, *Proc. Natl. Acad. Sci. U. S. A.*, 2007, **104**(23), 9656–9660.
72 J. Daillant, E. Bellet-Amalric, A. Braslau, T. Charitat, G. Fragneto, F. Graner, S. Mora, F. Rieutord and B. Stidder, *Proc. Natl. Acad. Sci. U. S. A.*, 2005, **102**(33), 11639–11644.
73 G. Fragneto and M. Rheinstaedter, *C. R. Phys.*, 2007, **8**(7–8), 865–883.
74 W. Feng, M. P. Nieh, S. Zhu, T. A. Harroun, J. Katsaras and J. L. Brash, *Biointerphases*, 2007, **2**, 34–43.
75 G. Tae, H. Yang, K. Shin, S. K. Satija and N. Torikai, *J. Pept. Sci.*, 2008, **14**(4), 461–468.
76 M. S. Kent, H. Yim, J. K. Murton, D. Y. Sasaki, B. D. Polizzotti, M. B. Charati, K. L. Kiick, I. Kuzmenko and S. Satija, *Langmuir*, 2008, **24**(3), 932–942.
77 E. Y. Chi, C. Ege, A. Winans, J. Majewski, G. Wu, K. Kjaer and K. Y. C. Lee, *Proteins: Struct., Funct., Bioinf.*, 2008, **72**(1), 1–24.